

Supporting information

Sb-MOFs Derived Sb Nanoparticles@Porous Carbon for High performance potassium-ion batteries anode

Na Cheng,^{‡ a,b} Jianguo Zhao,^{‡ c} Ling Fan,^a Zhaomeng Liu,^a Suhua Chen,^a Hongbo Ding,^a Xinzhi Yu,^a Zhigang Liu,^{b*} and Bingan Lu,^{a,d*}

Na Cheng, Prof. Jianguo Zhao, Dr. Ling Fan, Dr. Zhaomeng Liu, Dr. Suhua Chen, Hongbo Ding, Dr. Xinzhi Yu, Prof. Zhigang Liu, Prof. Bingan Lu

a School of Physics and Electronics, Hunan University, Changsha 410082, China

b School of Chemistry and Chemical Engineering, Hunan University, Changsha 410082, China

c School of Physics and Electronic Information, Luoyang Normal University, Luoyang, 471022, Henan, P. R. China

d Fujian Strait Research Institute of Industrial Graphene Technologies, Jinjiang, 362200, China

[‡] The authors contributed equally to this work.

*Corresponding author e-mail: liuzhigang@hnu.edu.cn; luba2012@hnu.edu.cn.

Experimental section

Reagents: The antimony metal organic frameworks (Sb-MOFs) were synthesized by using terephthalic acid as organic linker (TPA, 98%, Aldrich), antimony (III) chloride as metal ion sources (SbCl_3 , $\geq 99.0\%$, Sigma-Aldrich). potassium hydroxide (KOH, 99%, Sigma-Aldrich) was used to adjust the pH. Methanol (MeOH, 99.9%, Sigma-Aldrich) was used to solve the SbCl_3 . Ethanol (99.8%) was used for washing the Sb-MOFs and the distilled (DI) water was used throughout all the experiments.

Materials Preparation: The Sb-MOFs were synthesized by the previous literature.¹ And a few details have changed slightly. For the preparation of TPA solutions, 0.98g TPA were dissolved into 50 mL DI water and adjust the PH to 7 by addition of the 1mol/L KOH drop by drop. Separately, the metal ion solutions were prepared with 0.903g SbCl_3 into 50 mL MeOH. And then, the prepared metal ion solutions were added into the TPA solutions drop by drop. The mixture solutions of TPA and metal ion solution were agitated under magnetic stirring for 24 h at room temperature. After that, the Sb-MOFs were filtered with ethanol and DI water three times each before freeze drying. Finally, the synthesized Sb-MOF precursors were carbonized in an Ar/H_2 (90:10) atmosphere at 650°C for 4 hours with the heating rate of 3°C min^{-1} . After being carbonized, the samples were collected and stored for further characterizations and battery performance tests.

Electrochemical Measurements: Electrochemical measurements were performed using CR2032-type coin cells assembled in a glove box filled with pure Argon (Ar) filled gas ($\text{H}_2\text{O} < 0.5$ ppm, $\text{O}_2 < 0.5$ ppm). The potassium metal was used as cathode electrode, and 4 M solution of potassium bisv(fluorosulfonyl)imide (KFSI) in EMC as the electrolyte, the Whatman glass microfber filter was used as the separator. And the anode electrode was prepared with 80% of active materials, 10% of ketjen black, 10% of carboxyl methyl cellulose (CMC). The mass loading of the anode electrode was about (0.8 ± 0.2) mg cm^{-2} . And all the specific capacities were calculated based on the active materials. In order to ensure the full absorption of the

electrolyte to the electrode, all the cells were aged for at least 12 h to test. The galvanostatic charge-discharge measurements were tested by the battery testing system (Neware BTSCT-3008-TC 5.X, Shenzhen, China) with the voltage range of 0.01–2.6 V.

Characterization: The nanostructure and morphology of samples were observed by field-emission scanning electron microscopy (FESEM, Ultra 55, Zeiss, Germany) and transmission electron microscopy (TEM Titan G2 60-300). The crystal phases of the samples were identified by X-ray diffraction (XRD) (ULTIMA-3, Rigaku, Japan) recorded on Cu K α radiation ($\lambda = 0.154056$ nm) and operated at 40 kV and 40 mA. The X-ray photoelectron spectroscopy (XPS) analysis of the samples was conducted by ESCALAB 250Xi. Raman spectra were studied by Renishaw Raman Spectroscope with 532 nm laser as excitation source. The pore size distribution and specific surface area of the samples were measured by Brunauer-Emmett-Teller method (BET, Micromeritics ASAP2460). The mass contents of metal were confirmed by the thermogravimetric analysis (TGA, NETZSCH, STA449 F3). The cyclic voltammogram (CV) and the electrochemical impedance spectroscopy (EIS) were test by Electrochemical Workstation (CHI 660E, chenhua)

Materials	Cyclability	Capacity retention	Ref.
MXene@Sb	500 cycles at 500 mA/g	79.1435%	7
Sb/CNS	600 cycles at 200 mA/g	90%	6
Sb@CSN	100 cycles at 100 mA/g	94%	5
Sb-C-rGO	100 cycles at 500 mA/g	79%	2
Sb@G@C	800 cycles at 1000 mA/g	72.3%	4
NP-Sb	50 cycles at 100 mA/g	62.35%	3
Sb-NPs@PC	100 cycles at 100 mA/g	94.6%	This work

Table. S1 Electrochemical performance comparison of some reported Sb-based anodes of PIBs.

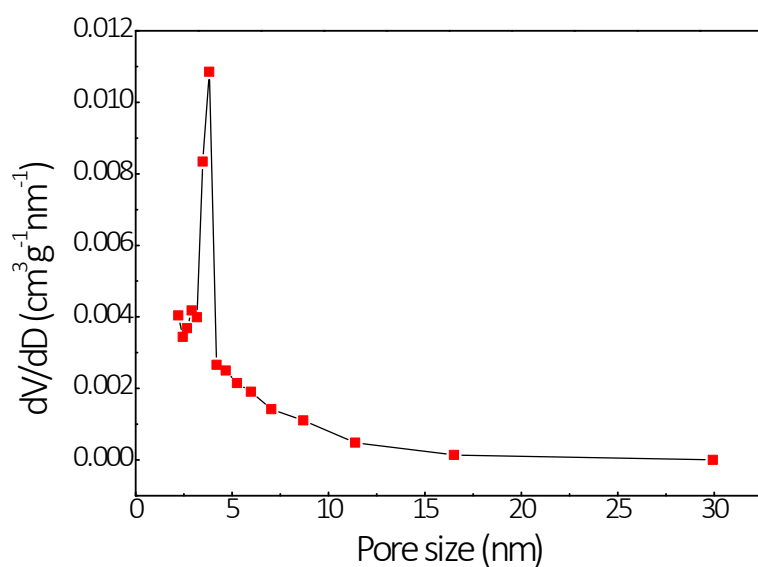


Fig. S1 BJH mesoporous and macropore pore size distribution of the Sb-NPs@PC sample.

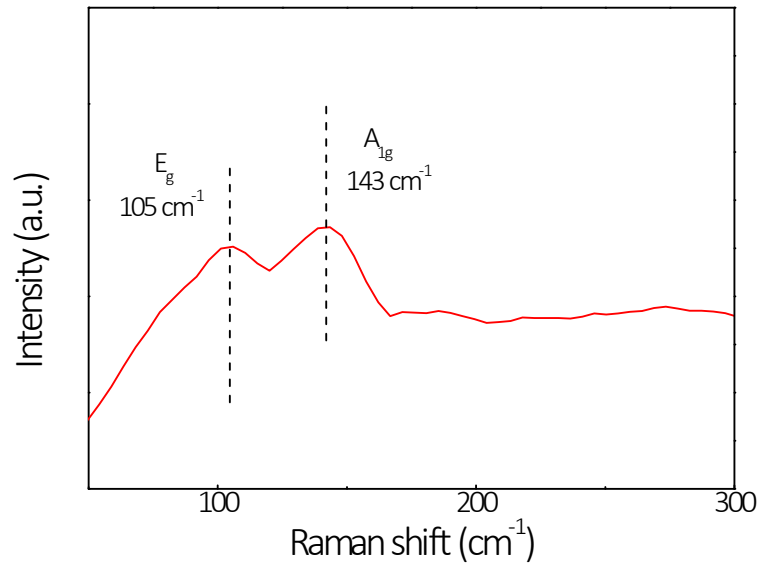


Fig. S2 Raman spectra of the Sb-NPs@PC sample.

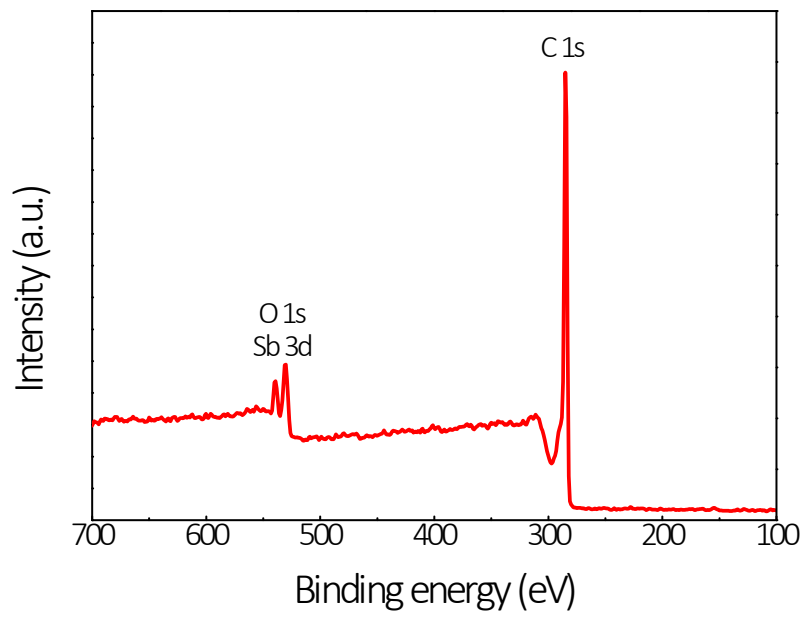


Fig. S3 The XPS survey scan spectra of the extracted Sb-NPs@PC sample.

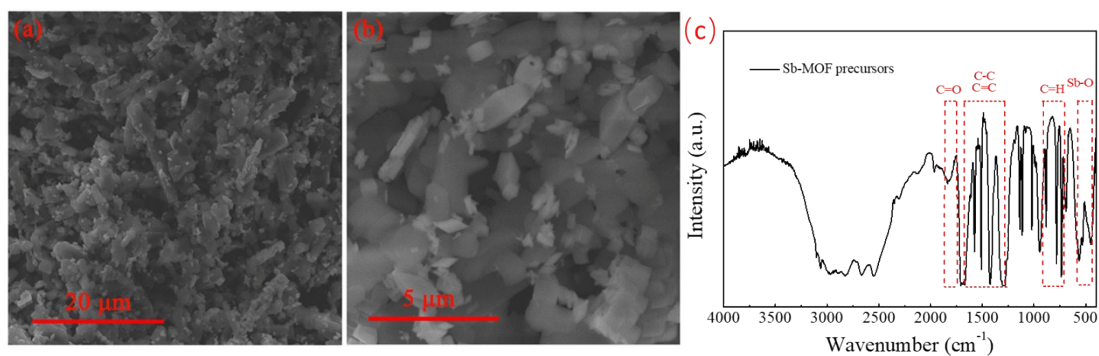


Fig. S4 Morphology of the Sb-MOF precursors. a,b) SEM images observed at 20 μm and 5 μm. c) FT-IR of Sb-MOFs precursors.

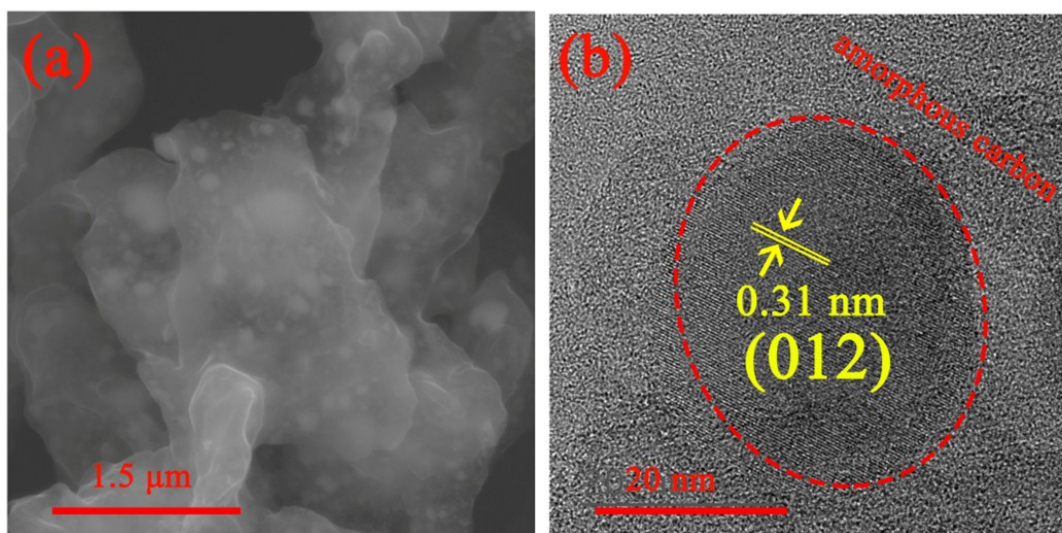


Fig. S5 Morphology of the Sb-NPs@PC sample. a) SEM images observed at 1.5 μm. b) High-resolution TEM image at 20nm.

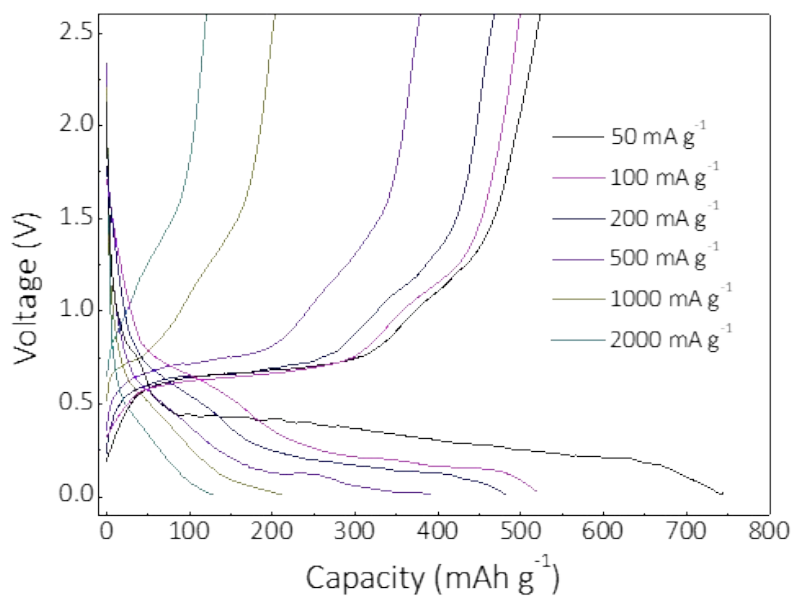


Fig. S6 The galvanostatic charge/discharge curves at different current density of 50, 100, 200, 500, 1000, 2000 mA g⁻¹.

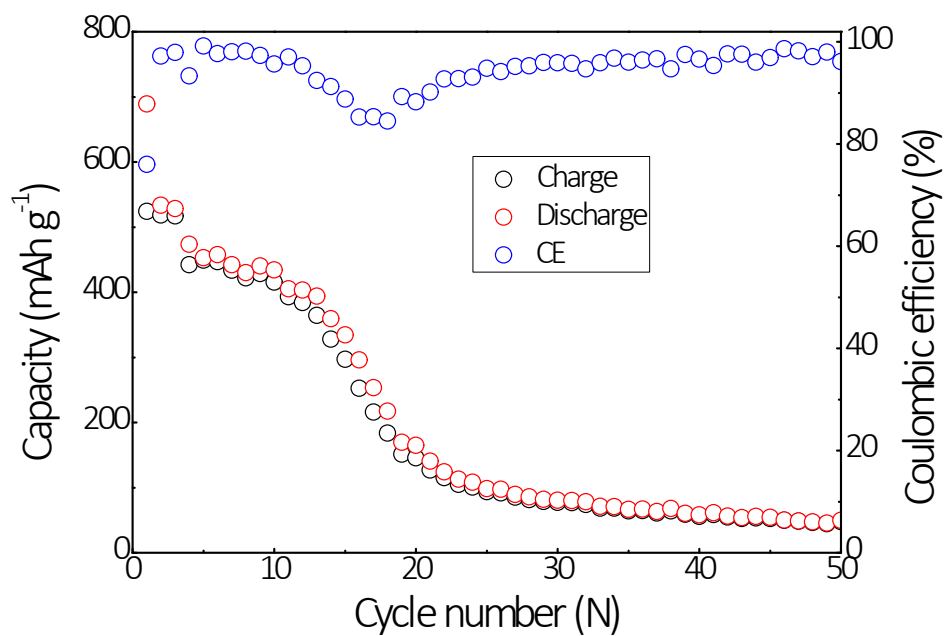


Fig. S7 Cycling performance of commercial Sb at the current density of 50 mA g⁻¹ (first three cycles) and 200 mA g⁻¹.

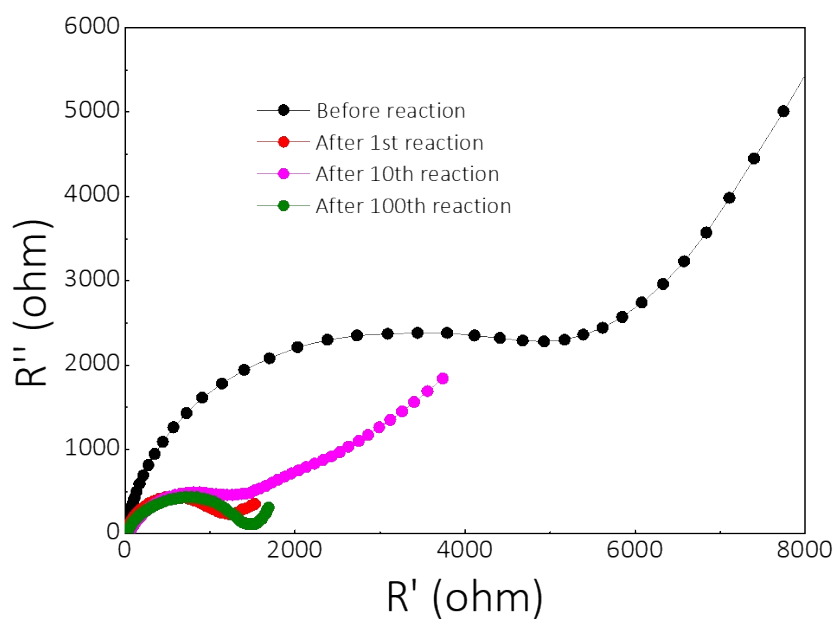


Fig. S8 Impedance spectra of the Sb-NPs@PC electrode material before reaction and after 1st, 10th, 100th cycles.

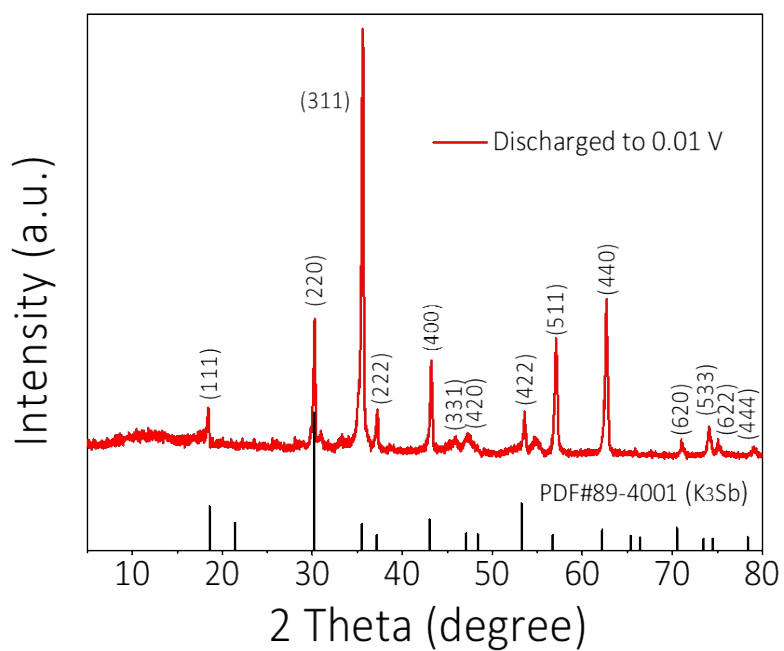


Fig. S9 XRD pattern of the Sb-NPs@PC electrode material at the discharged to 0.01V state.

Reference

1. N. Sahiner, S. Demirci, M. Yildiz, *Journal of Inorganic and Organometallic Polymers and Materials.*, 2017, **27**, 1333-1341.
2. Y. N. Ko, S. H. Choi, H. Kim, H. J. Kim, *ACS Appl Mater Interfaces.*, 2019.
3. Y. An, Y. Tian, L. Ci, S. Xiong, J. Feng, Y. Qian, *ACS Nano.*, 2018, **12**, 12932-12940.
4. Q. Liu, L. Fan, R. Ma, S. Chen, X. Yu, H. Yang, Y. Xie, X. Han, B. Lu, *Chem Commun (Camb)*. 2018, **54**, 11773-11776.
5. J. Zheng, Y. Yang, X. Fan, G. Ji, X. Ji, H. Wang, S. Hou, M. R. Zachariah, C. Wang, *Energy & Environmental Science.*, 2019, **12**, 615-623.
6. Y. Han, T. Li, Y. Li, J. Tian, Z. Yi, N. Lin, Y. Qian, *Energy Storage Materials.*, 2018, **20**, 46-54.
7. Y. Tian, Y. An, S Xiong, J. Feng, Y. Qian, *Journal of Materials Chemistry A.*, 2019, , 9716-9725.